Proceedings of ASME Turbo Expo 2020
Turbomachinery Technical Conference and Exposition
GT2020
September 21-25, 2020, Virtual, Online

GT2020-14733

INFLUENCE OF SPLITTER BLADES ON THE PERFORMANCE OF A SINGLE-STAGE CENTRIFUGAL COMPRESSOR WITH PRESSURE RATIO 12.0

Wenchao ZHANG[1], Zhenzhong SUN[2], Baotong WANG[2], Xinqian ZHENG*[1,2]

[1]Turbomachinery Laboratory, State Key Laboratory of Automotive Safety and Energy
Tsinghua University, Beijing, 100084, China.
[2]Institute for Aero Engine
Tsinghua University, Beijing, 100084, China.
Email: zhengxq@tsinghua.edu.cn

ABSTRACT

High performance centrifugal compressors with high pressure ratio are highly applied in turboshaft engines in order to obtain higher power-to-weight ratio and lower fuel consumption. The optimization of the aerodynamic configuration design of splitter blades is one of the effective ways to achieve higher efficiency. An in-house designed single-stage centrifugal compressor with a pressure ratio up to 12.0 is studied in this paper. By using a three-dimensional CFD (computational fluid dynamic) method, this paper investigates influences of the number of splitter blades and their leading edge position on the flow field characteristics and aerodynamic performance of the centrifugal compressor with ultra-high pressure ratio. Results show that three critical flow characteristics lead to severe losses in centrifugal compressor impeller when only full blades are applied. Those flow characteristics include the strong shock wave, the severe tip clearance flow at the inlet region and the severe flow separation at the rear region. Therefore, the inlet blade number should be reduced to decrease the loss caused by strong shock waves and tip clearance flow, while the outlet blade number should be sufficient enough to suppress flow separation. By optimizing the number and the leading edge position of splitters, the performance can be improved under the reduction of combined losses caused by shock waves, tip clearance flow and flow separation. When an aerodynamic configuration with single-splitters is used, numerical results indicate that the leading edge position of splitter blades should be located at 60% of the main blade chord length, and the centrifugal impeller isentropic efficiency with ultra-high pressure ratio can be increased from 82.4% (the aerodynamic configuration with only full blades) to 89.5%; when an aerodynamic configuration with double-splitters is used, the leading edge positions of middle and short splitter blades should be respectively located at 40% and 60% of the main blade chord length, and the impeller isentropic efficiency can be further improved to 90.9%.

NOMENCLATURE

m	Mass flow
B	Blade
C	Chord length
LE	Leading edge
Ma	Mach number
P_0	Total pressure
S	Leading edge position
Z	Blade number
π	Total-to-total pressure ratio
η	Total-to-total isentropic efficiency
subscripts	
m	Middle splitter blade
s	Splitter blade
1	Impeller inlet
2	Impeller outlet
4	Diffuser outlet

1. INTRODUCTION

Turboshaft engines are the main power units for helicopters due to their advantages of low fuel consumption, high power-to-weight ratio, and high reliability. Centrifugal compressors are the core components of turboshaft engines. The application of centrifugal compressors with high pressure ratio can further improve the fuel economy and power-to-weight ratio of the engine [1], which is considered to be the key technology of the

*Corresponding author

next-generation turboshaft engines. However, the efficiency of the compressor decreases and the flow phenomenon will deteriorate along with the increasing pressure ratio. Krain [2, 3, 4] of DLR (Deutsches Zentrum für Luft- und Raumfahrt) conducted numerical and experimental researches on the high pressure ratio transonic impeller with splitter blades named SRV2. The researches analyzed the influence of interaction between shock waves and boundary layers on the performance of compressors, which has laid the foundation for many research works on centrifugal impellers with high pressure ratio. Higashimori [5, 6] of MHI (Mitsubishi Heavy Industries) conducted an experimental study in a single-stage centrifugal compressor to investigate the flow phenomenon. The *Ma* near the LE of the impeller is as high as 1.6 and the pressure ratio of the compressor is up to 11.0. He pointed out that the reverse flow in the vicinity of casing surface is caused by the interaction of the shock wave and the blade tip clearance flow. Improving the internal flow field and aerodynamic performance is the major technical challenge with the increasing pressure ratio of centrifugal compressors, and the application of splitter blades is one of the effective methods which are widely applied into practice.

Researchers have been studying the splitter blades for a long time. As early as the 1980s, Fradin [7] investigated the performance of the impeller and it is concluded that the introduction of splitter blades can improve the flow field of the impeller and achieve better performance in a transonic centrifugal compressor. Millour [8] confirmed that the splitter blades contributed to reducing the load on the impeller blade and weakening the jet-wake loss near the trailing edge of the impeller by three-dimensional flow analysis. For two centrifugal compressors with and without splitter blades, Miyamoto [9] applied experimental methods to measure and analyze the internal flow fields, and pointed out that the secondary flow phenomenon in the impeller channel for the compressors with splitter blades was significantly reduced. Yamada [10] carried out a numerical study on centrifugal impellers with splitter blades and a design pressure ratio of 2.0. The results showed that a low momentum zone at the tip region of the blade enlarged rapidly with mass flow decreased. The tip clearance flow in this low momentum zone would be mixed with the mainstream near the LE region of splitter blades, eventually leading to a reduction of blade load and an increase of the flow loss at the tip region. In addition to single-splitter blades, double-splitter blades have also been researched with the continuous effort to improve the performance of compressors. According to Jawad [11], by comparing the aerodynamic configuration of single-splitters and double-splitters in a centrifugal compressor, it was found that the double-splitters could have the potential to further improve the performance and increase the flow capacity. Malik [12] improved the performance of the centrifugal compressor by using double-splitter blades with a pressure ratio equal to 4.0. The compressor isentropic efficiency was improved by 2% with more uniform outlet flow.

The LE position of splitter blades is a key parameter affecting impeller performance, and many researches have been deeply conducted on this issue. Lohmberg et al. [13] investigated a transonic compressor to determine the LE position of splitter blades. He explained that the LE of splitter blades should be placed far enough to avoid the blockage in the channel. Malik [14] introduced double-splitters to a centrifugal compressor, and conducted a study on the influence of LE positions for splitter blades when the pressure ratio of compressor is equal to 4.5. The results indicated that the design configuration of the middle splitter near the pressure surface and the short splitter near the suction surface of the main blade showed better performance with less separation loss. Moussavi [15] compared different LE positions of splitter blades in a centrifugal compressor with the pressure ratio of 2.4. The results showed that the impeller provided a 2.7% improvement in efficiency while maintaining the same pressure ratio when the LE of splitters was at 50% of the hub curve. The incidence angles by repositioning splitters is decreased and thus the related losses is minimized. Xu [16] reported that when the LE of the splitters was at the optimized position, the flow field performed more uniform at the impeller exit so as to improve the inlet condition of the diffuser. Omidi [17] also optimized the LE position of splitter blades, and finally increased the compressor efficiency by 2.5% with a pressure ratio equal to 2.25.

Most of the previous studies focused on centrifugal compressors with conventional pressure ratio. However, there are few related researches on the configuration of splitter blades for centrifugal compressors with ultra-high pressure ratio. Therefore, the impact of parameters such as the number and the LE position of splitters to improve the aerodynamic performance of an ultra-high pressure ratio centrifugal compressor are still unclear. This paper numerically investigated the effect of splitters configuration on the performance of a centrifugal compressor with ultra-high pressure ratio using an in-house designed single-stage centrifugal compressor with a total pressure ratio of 12.0 as the research object.

2. NUMERICAL METHODS AND VALIDATION

2.1 Case description

The datum design used in this study is an in-house developed single-stage centrifugal compressor and the design pressure ratio is equal to 12.0, which consists of an impeller and a vaned diffuser. This paper focuses on the flow field and performance in the impeller by introducing a vaneless diffuser since the splitter blades mainly have an important influence on the compressor impeller. The compressor specifications relating to the geometry are provided in Table 1, and the impeller schematic is presented in Fig. 1.

Table 1 Compressor specifications

PARAMETERS	VALUES
Number of impeller blades	36
Rotational Speed	57900 rpm

The LE tip radius	72.0 mm
The LE hub radius	29.0 mm
Radius at the impeller exit	112 mm
Width at the impeller exit	5.9 mm
Radius at the vaneless diffuser entrance	123.2mm
Radius at the vaneless diffuser exit	159.4mm
Width of the diffuser	5.4mm
Maximum impeller pressure ratio	13.7
Maximum impeller isentropic efficiency	82.4%

Fig. 1 Schematic diagram of the datum compressor impeller

2.2 Numerical methods

Fine/Turbo (NUMECA) [18] with the EURANUS solver is used for the three-dimensional and steady-state simulations. A finite volume method is applied to solve the compressible Reynolds-averaged Navier-Stokes equations. The temporal and spatial discretization are based on the fourth-order Runge-Kutta schemes [19] and the Jameson central scheme [20], respectively, and multi-grid techniques [21] are applied to accelerate the convergence. The turbulence model of the Spalart-Allamaras (SA) single equation [22] is selected and the perfect gas model in the software is chosen for the gas property.

The computational domain of the compressor is shown in Fig. 2(a). It can be divided into three regions: the inlet region, the impeller region and the vaneless diffuser region. The impeller region is meshed with O4H topology and the inlet and vaneless diffuser regions are meshed with H-type topology. The mesh of the inlet region consists of 73, 172 and 21 nodes in the spanwise, pitchwise and streamwise directions. For the impeller region, nodes are used in 73, 172 and 107, respectively. For the vaneless diffuser region, nodes are used in 73, 172 and 45, respectively. The inlet and impeller regions are simulated in the rotation frame of reference and the vaneless diffuser region is in the stationary frame of reference. The mixing-plane rotor-stator interface is placed between the impeller outlet and the diffuser inlet as shown in Fig. 2(a). The tip gap size is 0.17mm at impeller leading edge and 0.38mm at impeller trailing edge and the tip gap size changes linearly from leading edge to trailing edge. To fulfill the requirements from the SA turbulence model, 0.002mm is chosen for the cell width close to the wall. The scalar averaged y+ value is around 1.5 and the maximum y+ is less than 6 (shown in Fig. 2(b)) to precisely predict the flow in the boundary layer.

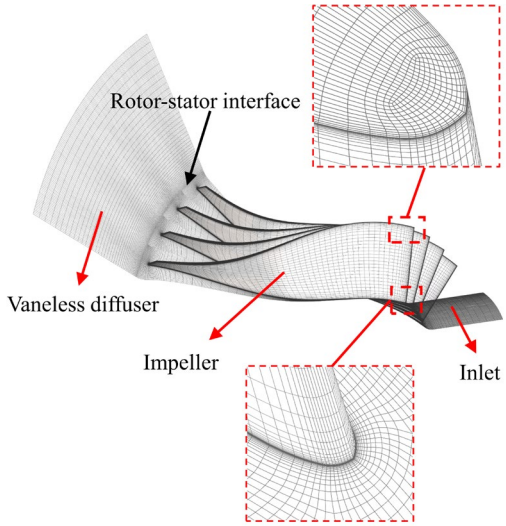

(a) Domains of the numerical model

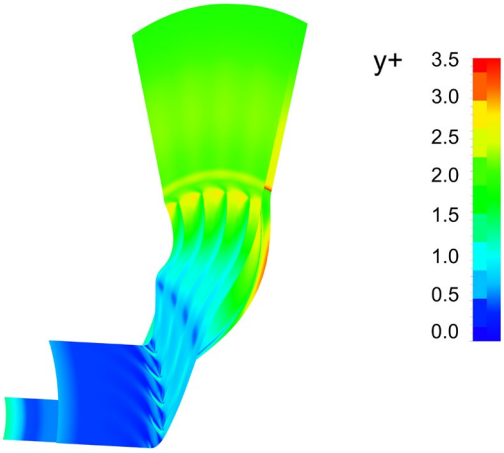

(b) y+ distribution

Fig. 2 Numerical methods: (a) domains of the numerical model; (b) y+ distribution

For the inlet boundary conditions, the total temperature and the total pressure are set to be 288.15 K, 101325 Pa, respectively, and the axial direction is specified to be the inlet flow direction. The static pressure is imposed as the outlet boundary condition to get the whole performance. The non-slip and adiabatic boundary conditions are set for the wall boundary. The step rise of the backpressure is set to be 1kPa at the near-surge condition. If the calculation cannot reach convergence under one backpressure after 10,000 iterations, it is considered that the mass flow corresponding to the previous backpressure is the surge boundary numerically predicted.

2.3 Numerical methods validation

A grid independent study was first conducted before investigating the parameter influence. The study investigated the compressor performance with the different number of nodes in the case of the same mesh topology, solver setting, turbulence model and boundary conditions. It can be found that the parameters show fine consistency when the grid number exceeds 2.2 million as illustrated in Fig. 3(a). The pressure ratio π_{14} and the isentropic efficiency η_{14} of the compressor are defined as the Equation (1) and (2). Therefore, the grid number of 2.9 million is adopted for exploration of the flow field and performance in the present study.

$$\pi_{14} = \frac{P_{04}}{P_{01}} \tag{1}$$

$$\eta_{14} = \frac{(\frac{P_{04}}{P_{01}})^{\frac{k-1}{k}} - 1}{\frac{T_{04}}{T_{01}} - 1} \tag{2}$$

The numerical methods have been verified on a centrifugal compressor named TTL-1 designed in Tsinghua University. The compressor in this paper is designed on the basis of TTL-1. The comparison results between the experiment(EXP) and CFD results of TTL-1 are presented in Fig. 3(b). The mass flow rate normalized by the choke mass flow is used to better compare the trend of the performance. The sufficient accuracy of numerical methods in this study can be validated since the error of the static pressure ratio is less than 2% between the EXP and CFD results. Further detailed information on the experimental test facility and the measuring sensor positions can be found in the work of He et al.[23]

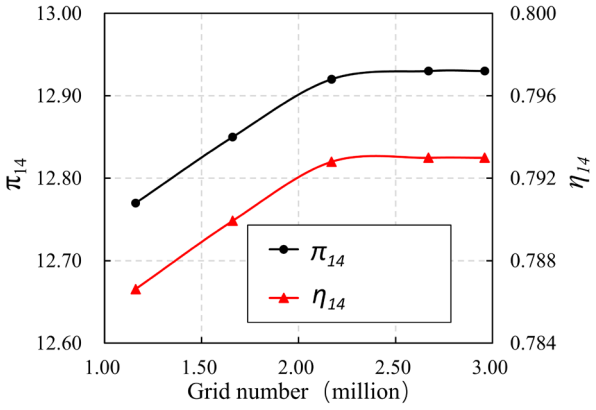

(a) Grid independent study

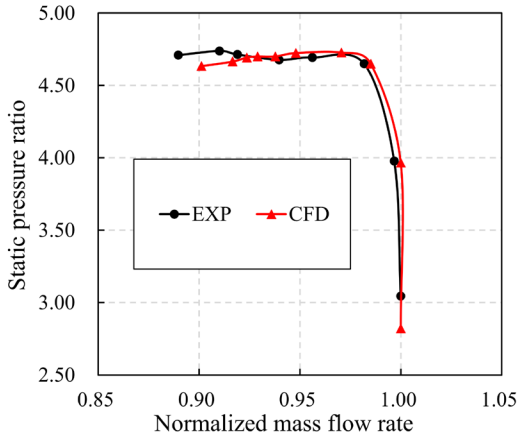

(b) Static pressure ratio of the TTL-1 impeller between the EXP and CFD results

Fig. 3 Validation of numerical methods

3. RESULTS AND ANALYSES

Three different aerodynamic configurations are studied in this section, consisting of configurations of only full-blades, single-splitters, and double-splitters as shown in Fig. 4. The impeller performance and flow field are analyzed for the purpose of clarifying the influence of two parameters, including the number and the LE position of splitters. The number of outlet blades for three aerodynamic configurations is selected to be 36 to make a fair comparison, and the influence of different blade numbers at the outlet will be stated in section 3.4.

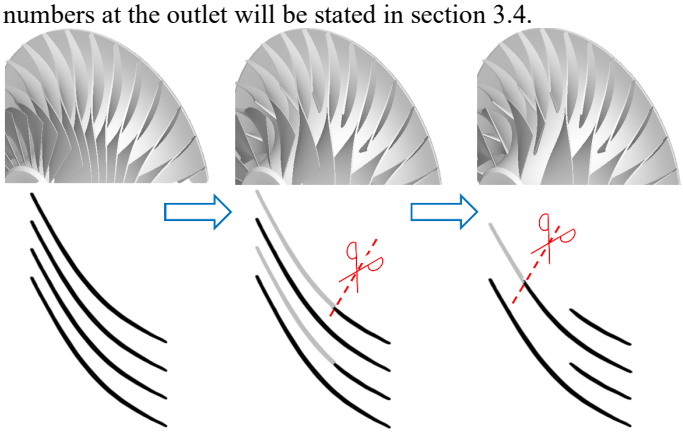

(a) Aerodynamic configuration with only full-blades

(b) Aerodynamic configuration with single-splitters

(c) Aerodynamic configuration with double-splitters

Fig. 4 Three blade aerodynamic configurations

3.1 Performance analysis of the aerodynamic configuration with only full-blades

For the compressor impeller with only full-blades, the performance maps are illustrated in Fig. 5. The impeller total pressure ratio π_{12} and the impeller isentropic efficiency η_{12} are defined as the Equation (3) and (4). The maximum pressure ratio of the datum impeller with only full-blades is 13.7 and the maximum isentropic efficiency is 82.4%, which indicates that

the centrifugal impeller with ultra-high pressure ratio needs to be optimized for improving its aerodynamic performance. Therefore, the flow field of the centrifugal impeller with only full-blades is analyzed to clarify loss mechanisms for the purpose of conducting an optimization design.

$$\pi_{12} = \frac{P_{02}}{P_{01}} \tag{3}$$

$$\eta_{12} = \frac{(\frac{P_{02}}{P_{01}})^{\frac{k-1}{k}} - 1}{\frac{T_{02}}{T_{01}} - 1} \tag{4}$$

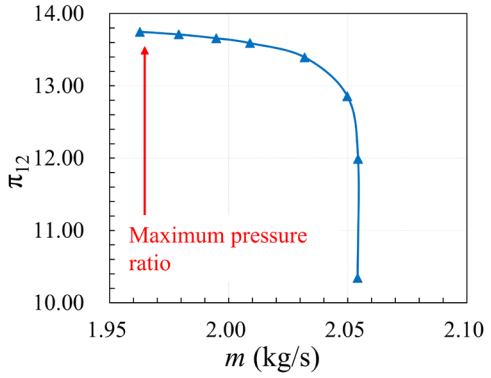

(a) Impeller total pressure ratio

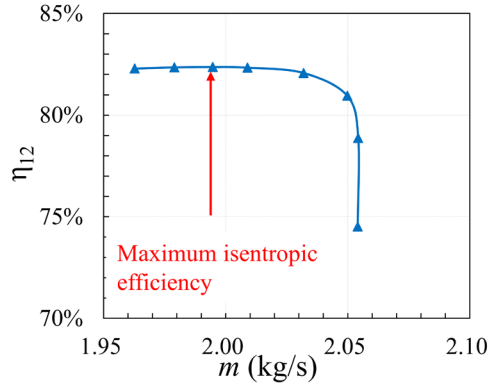

(b) Impeller isentropic efficiency

Fig. 5 Performance maps of the impeller with only full-blades

Figure 6 presents the entropy distribution along the streamwise. Two significant regions can be found with the entropy is rapidly increased, one region locating near the inlet region and the other locating near the rear region. Then the flow fields of the two regions are carefully investigated in order to find out the reason causing the severe flow losses.

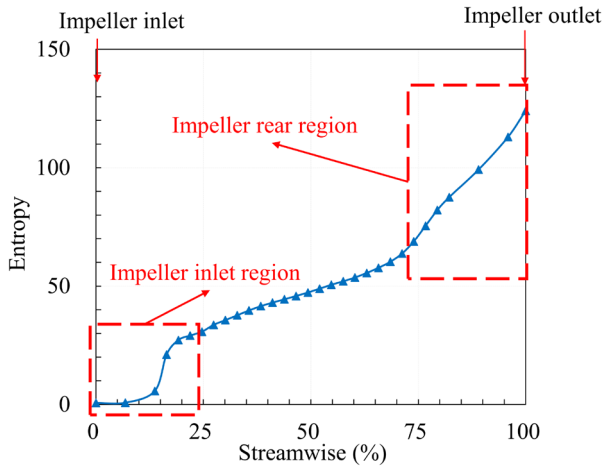

Fig. 6 Entropy distribution at peak efficiency point

Figure 7(a) shows the strong shock wave at the 90% span near the LE due to the high relative *Ma* at the impeller inlet (*Ma* > 1.6). Although the shock wave can result in the static pressure increase to a certain extent, the shock itself will cause significant flow loss, and the interactions, between the shock wave and the boundary layer [6] as well as the leakage flow [24], will also generate a large flow region with low momentum, significantly increasing the loss of the impeller. From the figure, a strong shock wave forms around the blade leading edge, which results in a significant loss at the inlet area. Fig. 7(b) illustrates the static pressure contour and the leakage flow near the impeller inlet. Severe tip leakage is presented in each channel at the inlet region by reason of the large pressure difference. The low-momentum fluids interfere with the mainstream fluids and the tip gas vortex is formed in the channel, which greatly increases the flow loss at the inlet region. In addition, high blade number at the impeller front region for the aerodynamic configuration with only full-blades further increases the losses corresponding to leakage vortices and decreases efficiency. As shown in Fig. 7(c), the phenomenon of severe flow separation occurs and deteriorates the flow field in the rear channel. Flow separation is also the main source of losses at the rear region of the impeller.

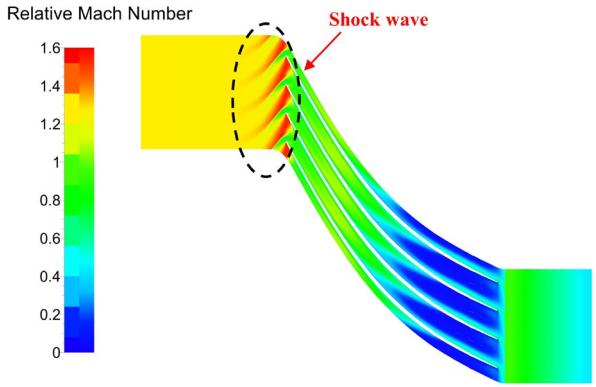

(a) Relative *Ma* contour at 90% span

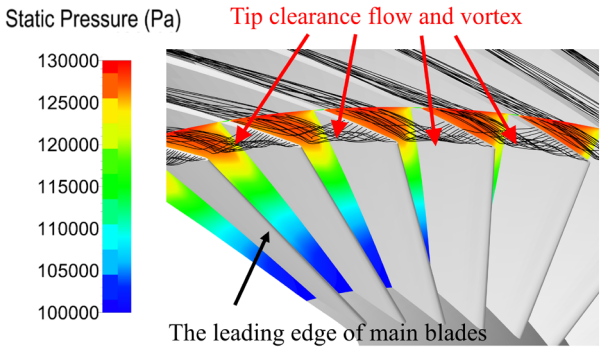

(b) Static pressure contour and tip clearance flow at the impeller inlet region

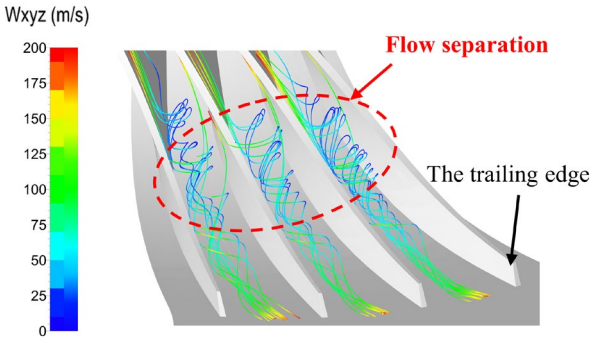

(c) Flow separation in the channel of the impeller

Fig. 7 The main source of losses for the impeller

According to the analysis above, strong shock wave, severe tip clearance flow at the inlet and severe flow separation in the rear channel are three main sources of losses for the centrifugal compressor impeller with ultra-high pressure ratio. The blade number has a contradictive effect on these three sources. The loss caused by inlet shock waves and tip clearance flow will increase with the increasing blade number. From this consideration, the blade number should not be excessive. However, the flow separation at the rear region of the channel will become severe with small blade number to increase the separation loss. Therefore, the blade number should not be too small in order to prevent the flow separation. It can come to the conclusion that the requirements of the blade number for the inlet region and the rear region of the centrifugal impeller with ultra-high pressure ratio are contradictive to bring a challenge for the compressor design.

3.2 Performance analysis of the aerodynamic configuration with single-splitters

In order to fulfill the different requirements for the blade number at inlet and rear regions of the centrifugal impeller with ultra-high pressure ratio, the datum full-bladed centrifugal impeller is modified and the aerodynamic configuration with single-splitters is adopted for the purpose of decreasing losses caused by the inlet strong shock waves and tip clearance flow and controlling the separation in the rear channel. The approach in this work is to keep the same outlet blade number and reduce the inlet blade number to half, as shown in Fig. 4(b).

3.2.1 Influence of the splitter LE position on the performance of the impeller with single-splitters

The aerodynamic configurations with different single-splitters LE positions are designed because the LE position of splitters can affect the flow loss caused by the surface friction and flow separation. In order to identify the different cases, the LE position parameter of single-splitters is defined in Equation (5)

$$S_s = \frac{C_{Main} - C_s}{C_{Main}} \tag{5}$$

C_s is the chord length of splitter blades, and C_{Main} is the chord length of main blades. The parameter $S_s = 60\%$ represents that the LE of splitter blades is formed by cutting the main blade at 60% position of the chord length. The higher S_s is, the further downstream is the leading edge position.

The cases with splitter LE positions S_s equal to 30%, 40%, 50%, 60% and 70% are investigated in detail. Fig. 8 shows the results of the peak efficiency of impellers and corresponding pressure ratio with five different LE positions. The impeller efficiency and pressure ratio reach the maximum with S_s equal to 60%. Therefore, the comparison of flow field will be made for the cases with S_s equal to 30%, 60% and 70% to further understand the influence of LE positions for spitter blades.

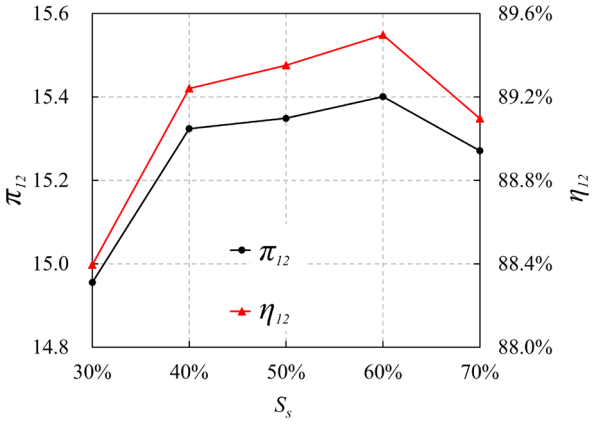

Fig. 8 Performance comparison at peak efficiency points with different splitter LE positions

When the splitter LE position changes from $S_s = 60\%$ to $S_s = 30\%$, the chord length of splitter blades becomes longer. The blade spacing is defined as presented in Fig. 9(a). The tip blade spacing distribution along the streamwise at the same mass flow is illustrated in Fig. 9(b). The tip blade spacing at the middle region of the channel is significantly reduced when $S_s = 30\%$, which means that impeller blades in the middle region of

channels are denser. Therefore, the increased blade surface area leads to increased friction loss and reduced impeller efficiency. When the splitter LE position changes from $S_s = 60\%$ to $S_s = 70\%$, the chord length of splitter blades is too small to well control separation. Although the friction loss is reduced, the capacity to suppress the flow separation at the impeller rear channel is weakened as shown in Fig. 10. For the case with S_s equal to 70%, the low momentum region in the middle channel enlarges significantly at 85% chord length, implying that flow separation becomes more severe at the impeller rear region, resulting in more severe loss and lower efficiency.

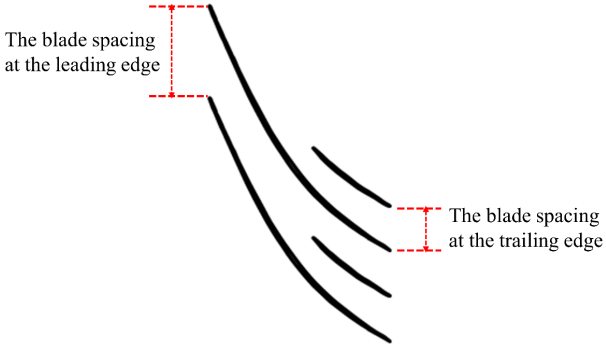

(a) The blade spacing

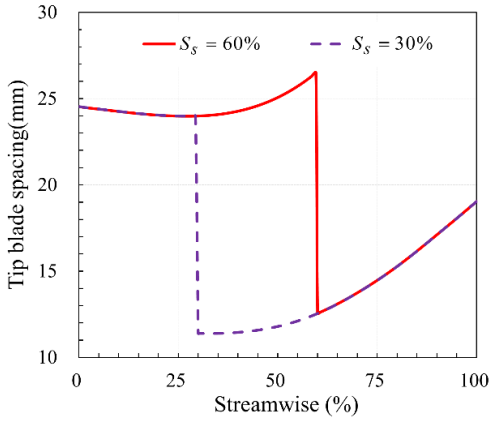

(b) Tip blade spacing distribution along with the streamwise direction

Fig. 9 Tip blade spacing distribution along with the streamwise direction with different splitter LE positions

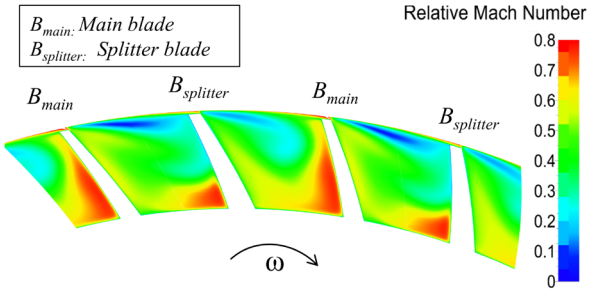

(a) $S_s = 60\%$

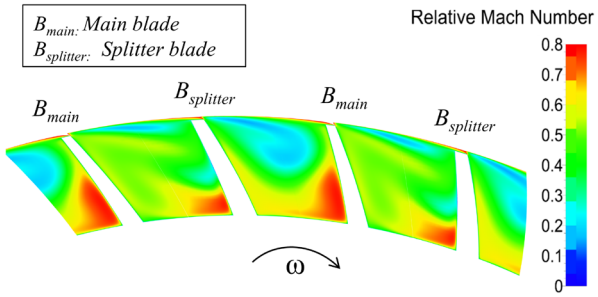

(b) $S_s = 70\%$

Fig. 10 Relative *Ma* distribution at 85% chord length of main blades with different splitter LE positions

From the analysis of the performance and flow field of compressors with different splitter LE positions, it can be concluded that different LE positions change the losses caused by the friction and separation. When S_s equals to 60%, the combined loss originated in the friction at the front region and separation in the rear channel of the impeller reaches the minimum, contributing to the maximum efficiency.

3.2.2 Performance of the single-splitters aerodynamic configuration

The performance of the impeller with single-splitters is compared to that with only full-blades, and the reasons for performance improving are analyzed. The splitter LE position is selected as $S_s = 60\%$.

When the single-splitters aerodynamic configuration is adopted, the impeller performance maps are presented in Fig. 11. Compared with the full-bladed aerodynamic configuration, all the pressure ratio, the efficiency and the flow capacity are increased. The choke mass flow rate and the maximum pressure ratio are improved by 23.5% and 11.5%, respectively. The maximum efficiency is increased from 82.4% to 89.5%.

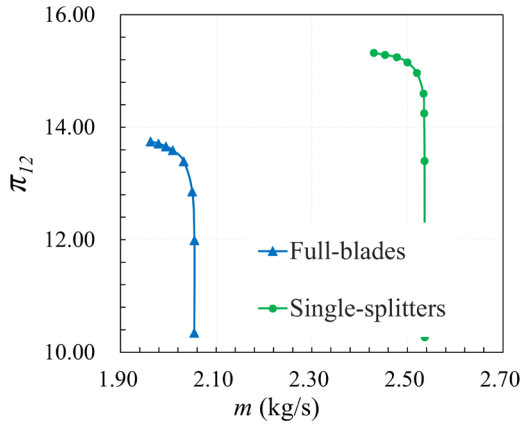

(a) Impeller total pressure ratio

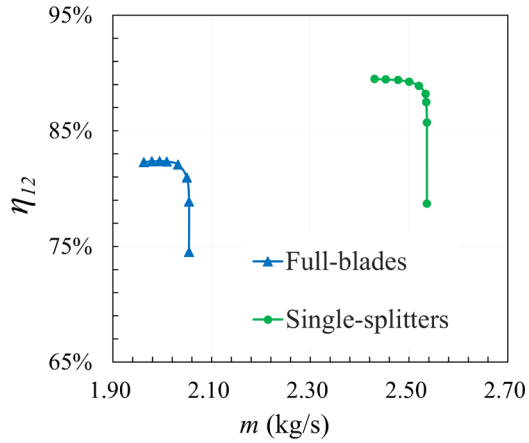

(b) Impeller isentropic efficiency

Fig. 11 Performance maps of two different aerodynamic configurations

In order to further understand the reasons for the improvement in efficiency, the flow fields of two configurations are compared in detail in Fig. 12. The results of the full-bladed aerodynamic configuration are shown on the figures above and the results of the single-splitters aerodynamic configuration are shown on the figures below. Figure 12(a) presents the contour of the relative *Ma* at 90% span. Although the maximum *Ma* has not reduced, the number of inlet shock waves has decreased due to decreased inlet blade number, resulting in decreased flow loss. The comparison of the tip clearance flow is illustrated in Fig. 12(b). Firstly, the channel number is reduced and the number of tip clearance flow is decreased. Also, because blades in the front region become sparse, the leakage flow does not interfere with the mainstream near the pressure surface of neighboring blades. No obvious vortex is formed at the inlet. The loss originated in the tip clearance flow is decreased. In addition, since the blade number at the impeller front region is reduced, the surface friction loss is also decreased. The *Ma* distributions at the rear region of two different aerodynamic configurations are illustrated in Fig. 12(c). The low-momentum region at different cross flow sections along the streamwise directions is significantly shrunk. Therefore, the introduction of splitters can effectively control the flow separation in the impeller rear region.

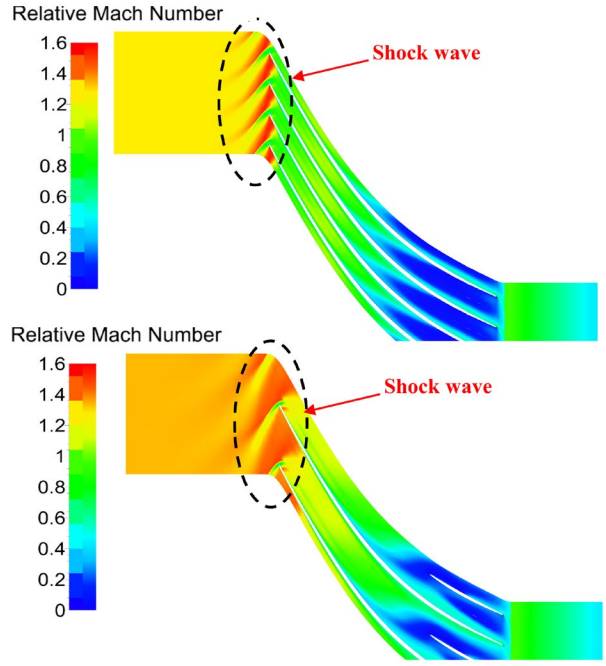

(a) Relative *Ma* contour at 90% span: full-blades(above); single-splitters(below)

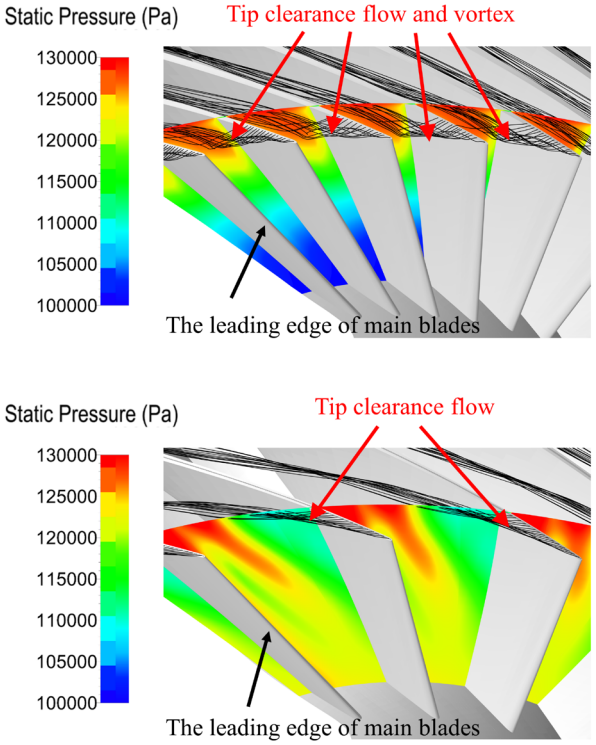

(b) Static pressure contour and tip clearance flow at impeller inlet region: full-blades(above); single-splitters(below)

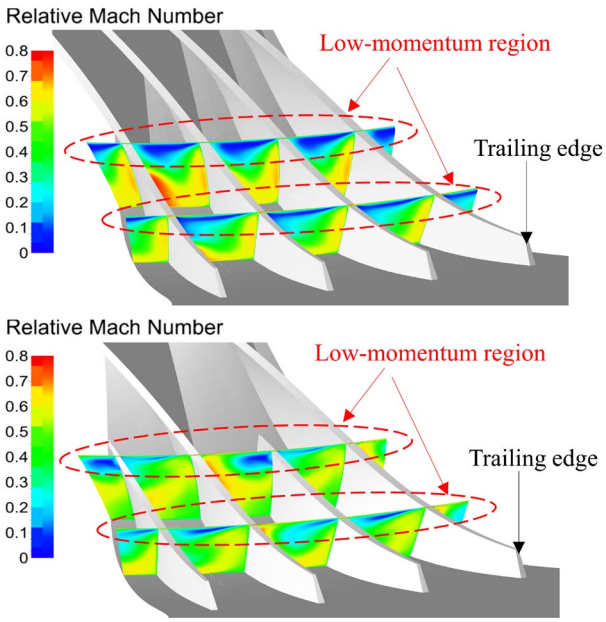

(c) Relative *Ma* contours at different cross flow sections: full-blades(above); single-splitters(below)

Fig. 12 Comparison of the flow field of two different aerodynamic configurations at peak efficiency point

Combining the factors above, the flow fields at the impeller inlet and rear regions with single-splitters aerodynamic configuration are improved significantly, and the corresponding losses are reduced. It can be seen from Fig. 13 that the entropy increase at both the impeller inlet region and the rear region decreases to some extent. Therefore, compared with aerodynamic configuration with only full-blades, the combined losses caused by shock waves, tip clearance flow and surface friction in the front channel and flow separation at the rear region are minimized to achieve higher impeller performance by introducing the single-splitters aerodynamic configuration.

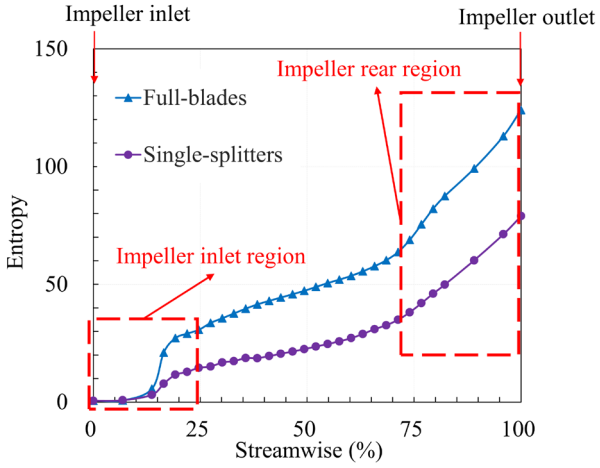

Fig. 13 Entropy distribution along with the streamwise direction of two different aerodynamic configurations

3.3 Performance analysis of the aerodynamic configuration with double-splitters

To further decrease the loss at the front region of the single-splitters aerodynamic configuration, a double-splitters aerodynamic configuration is proposed. The method in this study is to reduce the inlet blade number to half again and keep outlet blade number the same, as shown in Fig. 4(c). The shortened main blade is named the middle blade, and the original splitter blade is named the short blade. The LE position of short blades still remains with S_s equal to 60%.

3.3.1 Influence of the LE position of middle blades on the performance of the impeller with double-splitters

Different LE positions of middle blades can also make a difference in aerodynamic performances and flow field of the impeller. Therefore, to identify different cases, the parameter of the LE position of middle blades is also defined as:

$$S_m = \frac{C_{Main} - C_m}{C_{Main}} \tag{6}$$

C_{Main} is the chord length of main blades and C_m is the chord length of middle blades. The higher S_m is, the further downstream is the leading edge position.

The results of four different cases with S_m equal to 20%, 30%, 40% and 50% are compared. The selection of S_m is based on two reasons. One is that the chord length of middle blades is always longer than that of short blades and the other is that the changes of S_m do not change the choke mass flow rate of the compressor. The resulting pressure ratio and efficiency of the impeller at the peak efficiency point are presented in Fig. 14. The impeller with S_m equal to 40% obtains the maximum efficiency and pressure ratio. The flow fields of cases with S_m equal to 20% and 50% are compared with that of the case with S_m equal to 40%, respectively, to further understand the parameter effect of LE positions for middle blades.

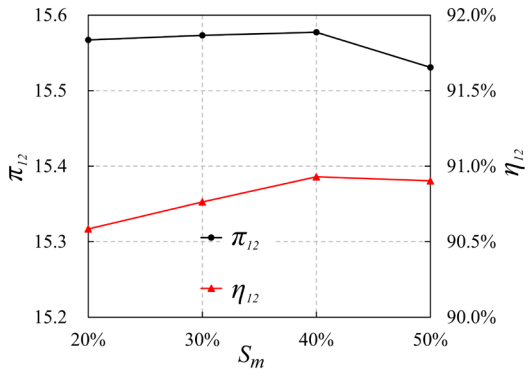

Fig. 14 Performance comparison at peak efficiency points with different LE positions of middle blades

When the LE position of middle blades is adjusted from $S_m = 40\%$ to $S_m = 20\%$, the chord length of middle blades

becomes larger. First, the friction loss increases due to the increased blade surface area. Also, a shock wave will be generated on the suction surface when fluids flow through the leading edge of middle blades because the fluids have not slowed down to a sufficiently low speed in the case with S_m equal to 20%, as shown in Fig. 15. Therefore, the corresponding loss caused by the shock waves is increased. Taking the above two points into consideration, the loss of the impeller front region will increase and the efficiency will decrease. When the LE position of middle blades is changed from $S_m = 40\%$ to $S_m = 50\%$, the flow separation in the channel cannot be suppressed well. As illustrated in Fig. 16, at 70% chord length of main blades, the low-momentum region in the impeller channel is significantly enlarged, indicating the flow separation is more severe in the impeller rear region. The efficiency still drops even though the friction loss is reduced.

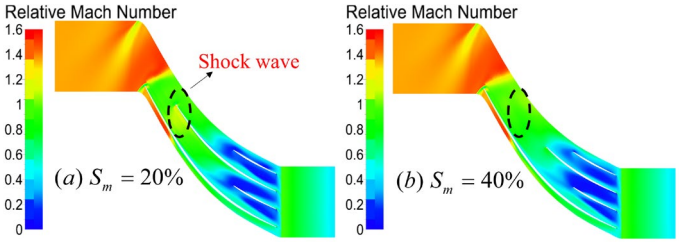

Fig. 15 Relative *Ma* contour at 90% span with different LE positions of middle blades

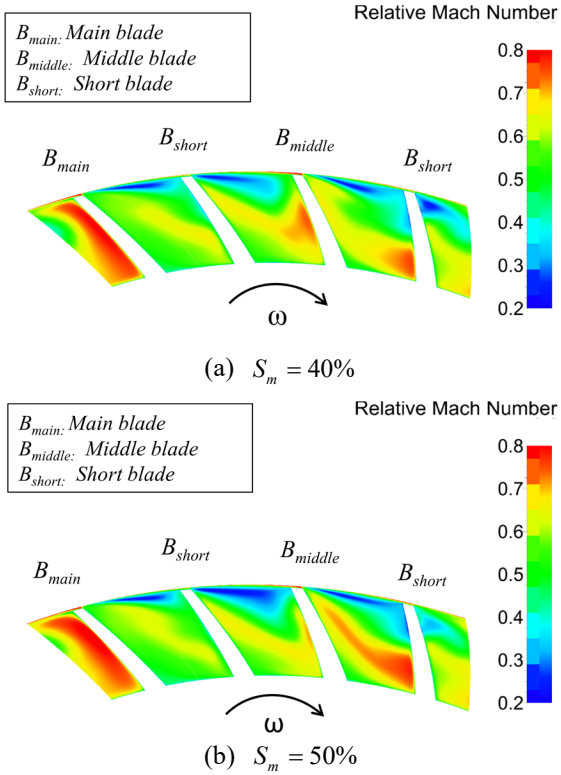

Fig. 16 Relative *Ma* distribution at 70% chord length of main blades with different LE positions of middle blades

If the LE position of middle blades is too close to the LE of main blades, the shock loss and friction loss at the impeller front region will be increased. If the LE position of middle blades is too far from the LE of main blades, the flow separation at the impeller rear region cannot be well suppressed. Therefore, in the case with S_m equal to 40%, the combined losses caused by the shock waves, friction, and flow separation are minimized and the impeller efficiency reaches the optimized value.

3.3.2 Performance of the double-splitters aerodynamic configuration

The performance maps of three aerodynamic configurations are illustrated in Fig. 17. For impeller with double-splitters, the LE positions of middle blades and short blades are chosen to be $S_m = 40\%$ and $S_s = 60\%$, respectively. The flow capacity, the pressure ratio and the efficiency are further increased when the double-splitters aerodynamic configuration is adopted. Compared with the single-splitters aerodynamic configuration, the maximum pressure ratio and choke mass flow rate are improved by 1.6% and 6.0%, repectively. Moreover, the maximum efficiency is increased from 89.5% to 90.9%.

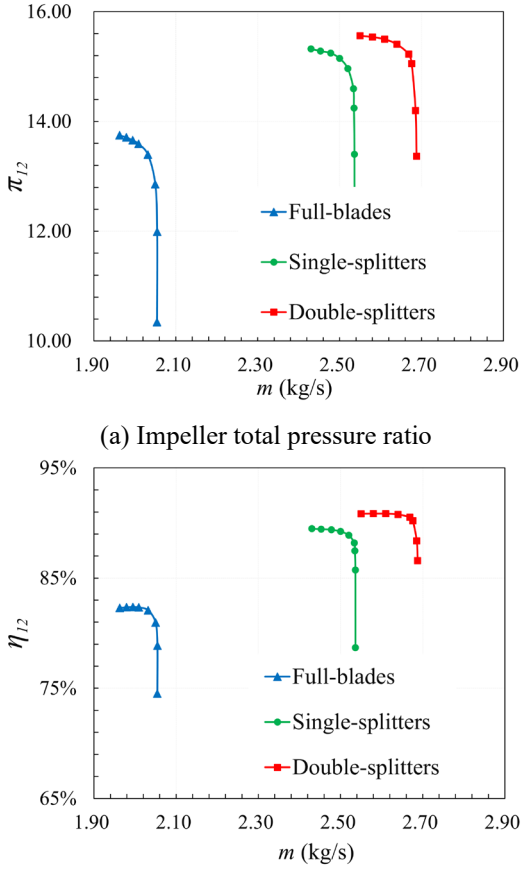

Fig. 17 Performance maps of three different aerodynamic configurations

The flow field is investigated in detail to analyze the mechanism of the double-splitters aerodynamic configuration to further reduce the loss. The shock waves and tip clearance flow at the inlet region of impeller are portrayed in Fig. 18(a) and Fig. 18(b). Compared to Fig. 12(a) and Fig. 12(b), the number of the shock waves and tip clearance flow is further decreased at inlet region, which results in decreased losses. Moreover, the blade number of the front region is reduced to improve the surface friction loss. The *Ma* contours at different cross flow sections along the streamwise directions are illustrated in Fig. 18(c). The effect of splitters on suppressing the flow separation is presented. The low momentum region near the shroud has been shrunk by introducing both the single-splitters and the double-splitters from Fig. 12(c) and Fig. 18(c). This flow phenomenon is related to the improvement of flow separation, resulting in loss reduction and efficiency increase. Compared to the single-splitters aerodynamic configuration, the low momentum region of the double-splitters configuration slightly enlarges due to the shorten middle blades.

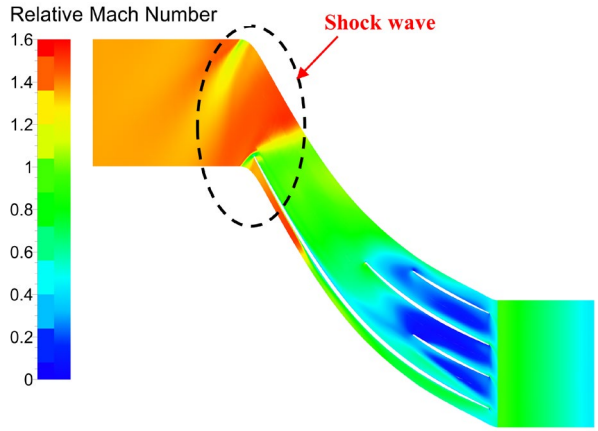

(a) Relative *Ma* contour at 90% span

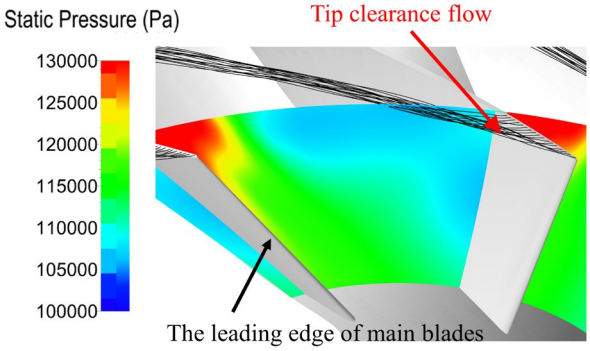

(b) Static pressure contour and tip clearance flow at impeller inlet region

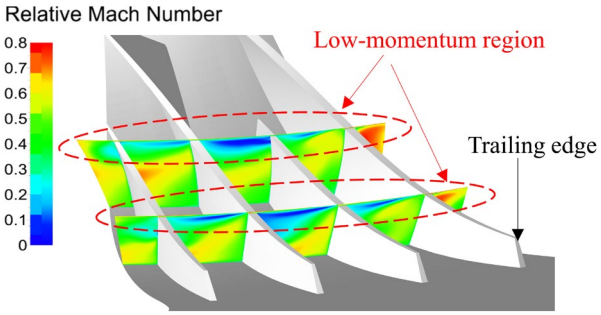

(c) Relative *Ma* contours at different cross flow sections

Fig. 18 The flow field of the aerodynamic configuration with double-splitters at peak efficiency point

The entropy distribution along the streamwise direction of three different aerodynamic configurations with only full-blades, single-splitters and double-splitters is shown in Fig. 19. It can be found that the entropy increase at the inlet region is decreasing by increased number of splitter blades with keeping the same outlet blade number, confirming that splitters can optimize the flow at the impeller inlet region. The improvement by introducing the double-splitters aerodynamic configuration is better than that of the single-splitters. Moreover, splitter blades are also effective in controlling the separation at the rear region of the impeller, leading to reduced flow losses.

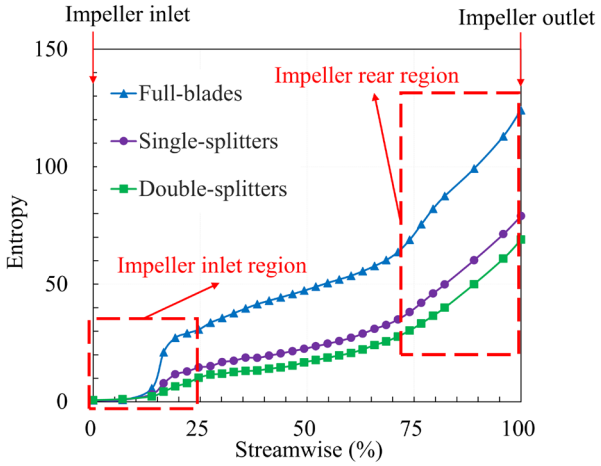

Fig. 19 Entropy distribution along with the streamwise direction of three aerodynamic configurations

Compared to the aerodynamic configuration with single-splitters, when the double-splitters configuration is introduced, the losses originated in the shock waves, tip clearance flow and friction at the inlet region are significantly reduced. Therefore, the combined loss is further suppressed to improve the impeller efficiency.

3.4 Selection of blade number

The blade number of compressors used in this research is 36. From the perspective of performance, in order to confirm if this selection of blade number is reasonable, the efficiency and pressure ratio of impellers with double-splitters are illustrated in

Fig. 20 when the outlet blade number is different. As presented in Fig. 20, the choke flow rate decreases by increasing the blade number. When the blade number is 36, the impeller pressure ratio and the efficiency reach the maximum. Therefore, it is reasonable to choose the blade number to be 36.

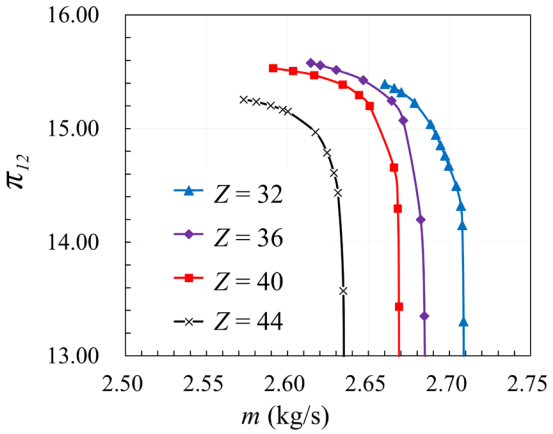

(a) Impeller pressure ratio

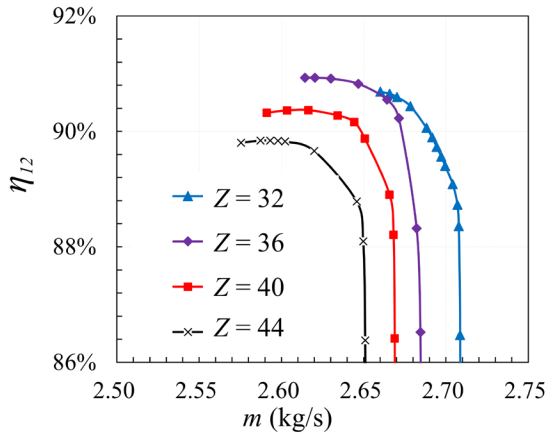

(b) Impeller efficiency

Fig. 20 Performance maps for different blade numbers

4. CONCLUSIONS AND REMARKS

This paper studies an in-house designed single-stage centrifugal compressor with a pressure ratio 12.0, and the influence of aerodynamic configurations of splitter blades on the compressor performance is numerically investigated. Several conclusions are obtained as follows:

(1) The strong shock waves, the severe tip clearance flow at the inlet region and the heavy flow separation at the rear region are three main loss sources of the centrifugal compressor impeller with ultra-high pressure ratio. The blade number should be limited due to the requirement for reducing the number of strong shock waves and tip clearance flow at inlet region, while the blade number should not be too small due to the requirement for suppressing the severe flow separation at rear region. This contradiction has brought challenges to the aerodynamic design of centrifugal compressors with ultra-high pressure ratio. Splitter blade is an effective technology to deal with this challenge, and the number and the LE position of splitter blades are two critical parameters for the impeller design with splitter blades.

(2) When the aerodynamic configuration with single-splitters is used for the impeller, the performance is optimal when the LE of splitter blades is located at 60% of the chord length of main blades. Compared to the aerodynamic configuration with only full-blades, the impeller efficiency is increased from 82.4% to 89.5%. The losses caused by the shock waves, tip clearance flow and surface friction at the impeller front region are improved and the flow separation in the rear region is suppressed.

(3) Based on the aerodynamic configuration with single-splitters, the aerodynamic configuration with double-splitters is introduced for the impeller. Results show that the impeller performance is optimal when the LE positions of middle blades and short blades are located at 40% and 60% of the chord length of main blades, respectively. Compared with the aerodynamic configuration with single-splitters, the impeller efficiency is increased from 89.5% to 90.9%. The losses caused by the shock waves, tip clearance flow and surface friction at the impeller front region are further reduced, resulting in decreased loss and improved impeller efficiency.

ACKNOWLEDGMENTS

This research was supported by National Science and Technology Major Project (2017-II-0002-0014), and the Tsinghua University "Shuimu Tsinghua Scholar" Program.

REFERENCES

[1] Krain, H., 2005, "Review of Centrifugal Compressor's Application and Development," ASME J. Turbomach., **127**(1), pp. 25-34.

[2] Krain, H., Hoffmann, B., and Pak, H., 1995, "Aerodynamics of a Centrifugal Compressor Impeller with Transonic Inlet Conditions," ASME Paper No. 95-GT-79.

[3] Eisenlohr, G., Krain, H., Richter, F. A., and Tiede, V., 2002, "Investigations of the Flow through a High Pressure Ratio Centrifugal Impeller," ASME Paper No. GT2002-30394.

[4] Krain, H., and Hoffmann, B., 2008, "Flow Study of a Redesigned High-Pressure-Ratio Centrifugal Compressor," J. Propul. Power., **24**(5), pp. 1117-1123.

[5] Higashimori, H., Hasagawa, K., Sumida, K., and Suita, T., 2004, "Detailed Flow Study of Mach Number 1.6 High Transonic Flow with a Shock Wave in a Pressure Ratio 11 Centrifugal Compressor Impeller," ASME J. Turbomach., **126**(4), pp. 473-481.

[6] Higashimori, H., Morishita, S., Suzuki, M., and Suita, T., 2007, "Detailed Flow Study of Mach Number 1.6 High Transonic Flow in a Pressure Ratio 11 Centrifugal Compressor Impeller: Part 2 - Effect of the Inducer Shroud Bleed and Development of a Low Energy Region along the Shroud," ASME Paper No. GT2007-27694.

[7] Fradin, C., 1987, “Investigation of the Three-Dimensional Flow near the Exit of Two Backswept Transonic Centrifugal Impellers,” Proc. of the Eighth International Symposium in Air Breathing Engines, pp. 149-155.
[8] Millour, V., 1988, “3D Flow Computations in a Centrifugal Compressor with Splitter Blade Including Viscous Effect Simulation,” In:16th Congress, International Council for Aeronautical Societies, **1**, pp. 842-847.
[9] Miyamoto, H., and Nakashima, Y., 1992, “Effects of Splitter Blades on the Flows and Characteristics in Centrifugal Impeller,” JSME International Journal, **35**(2), pp. 238-246.
[10] Yamada, K., Tamagawa, Y., Fukushima, H., Furukawa, M., Ibaraki, S., and Iwakiri, K. I., 2010, “Comparative Study on Tip Clearance Flow Fields in Two Types of Transonic Centrifugal Compressor Impeller with Splitter Blades,” ASME Paper No. GT2010-23345.
[11] Jawad, L. H., Abdullah, S., Zulkifli, R., and Mahmood, W. M. F. W., 2012, “Numerical Simulation of Flow inside a Modified Turbocharger Centrifugal Compressor,” Asian J. Appl. Sci., **5**(8), pp. 563-572.
[12] Malik, A., Qureshi, S. R., Zheng, Q., and Ikram, N., 2018, “Aerodynamic Analysis of Splitter Blade Location on Centrifugal Compressor Performance,” In 2018 8th International Conference on Power and Energy Systems (ICPES), Colombo, Sri Lanka, pp. 207-211.
[13] Lohmberg, A., Casey, M., and Ammann, S., 2003, “Transonic Radial Compressor Inlet Design,” Proc. Ins. Mech. Eng., Part A, **217**(4), pp. 367-374.
[14] Malik, A., and Qun, Z., 2019, “Effect of Double Splitter Blades Position in Centrifugal Compressor Impeller,” Proc. Inst. Mech. Eng., Part A, **233**(6), pp. 689-701.
[15] Moussavi, S. A., Benisi, A. H., and Durali, M., 2017, “Effect of Splitter Leading Edge Location on Performance of an Automotive Turbocharger Compressor,” Energy, **123**, pp. 511-520.
[16] Xu, C., and Amano, R. S., 2018, “Centrifugal Compressor Performance Improvements Through Impeller Splitter Location,” J. Energy Resour. Technol., **140**(5), 051201.
[17] Omidi, M., Liu, S. J., Mohtaram, S., Lu, H. T., and Zhang, H. C., 2019, “Improving Centrifugal Compressor Performance by Optimizing the Design of Impellers Using Genetic Algorithm and Computational Fluid Dynamics Methods,” Sustainability, **11**(19), pp. 5409.
[18] NUMECA International, 2015, “*NUMECA FINE/Turbo User Manual 10.1*”, http://www.numeca.com.
[19] Jameson, A., Schmidt, W., and Turkel, E., 1981, “Numerical Solutions of the Euler Equations by Finite Volume Methods Using Runge-Kutta Time-Stepping Schemes,” AIAA Paper No. 81-1259.
[20] Jameson, A., and Baker, T., 1981, “Solution of the Euler Equations for Complex Configurations,” AIAA Paper No. 81-1259.
[21] Martinelli, L., 1987, “Calculations of Viscous Flows with a Multigrid Method,” Ph.D. Thesis, Princeton University, USA.
[22] Spalart, P., and Allmaras, S., 1992, “A One-Equation Turbulence Model for Aerodynamic Flows,” AIAA Paper No. 92-0439.
[23] He, X., and Zheng, X., 2019, “Roles and Mechanisms of Casing Treatment on Different Scales of Flow Instability in High Pressure Ratio Centrifugal Compressors,” Aerosp. Sci. Technol., **84**, pp. 734-746.
[24] Seiichi, I., and Masato, F., 2007, “Vortical Flow Structure and Loss Generation Process in a Transonic Centrifugal Compressor impeller,” ASME Paper No. GT2007-27791.